



Occurrence and health risks of tire-derived chemicals in urban road dust

Rong Hu^{1,2}, Yue-Hong Liu¹, Xiang-Ning Liang¹, Hai-Yan Zhang¹, Zheng Huang¹, Zi-Tong Li¹, Li-Qian Lin¹, Jian-Liang Zhao^{1,2,3} , Guang-Guo Ying^{1,2,3}

Keywords:

Tire-derived chemicals, road dust, *in silico* toxicity prediction, priority pollutants

Citation: Hu, R.; Liu, Y. H.; Liang, X. N.; Zhang, H. Y.; Huang, Z.; Li, Z. T.; Lin, L. Q.; Zhao, J. L.; Ying, G. G. Occurrence and health risks of tire-derived chemicals in urban road dust. *J. Environ. Expo. Assess.* 2026, 5, 17. <https://dx.doi.org/10.20517/jeea.2026.03>

Received: 13 Jan 2026

First Decision: 28 Feb 2026

Revised: 2 Apr 2026

Accepted: 29 Apr 2026

Published: 25 May 2026

Academic Editor:

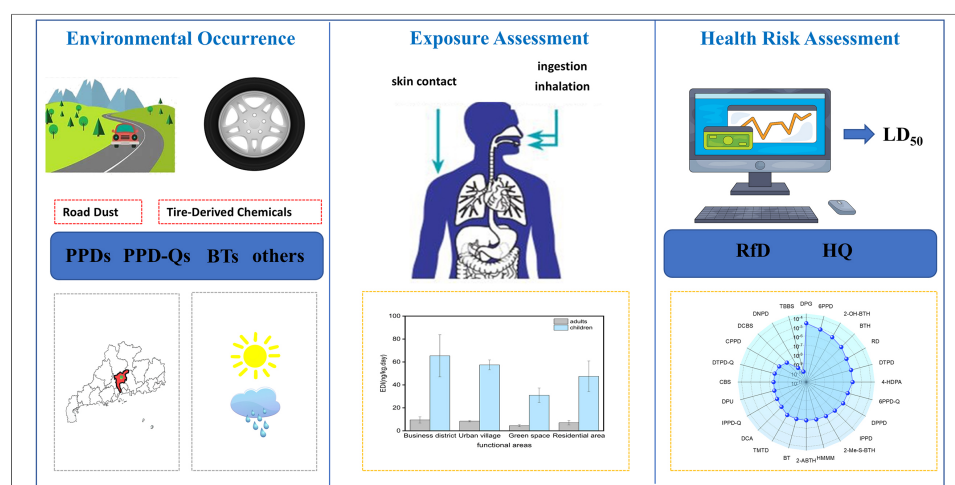
Giulia Poma

Copy Editor:

Pei-Yun Wang

Production Editor:

Pei-Yun Wang



Abstract

Despite the widespread presence of tire-derived chemicals (TDCs) in the environment, research on their occurrence in road dust and the associated health risks remains limited. This study quantified 30 TDCs in 24 seasonal road dust samples collected from four functional areas in Guangzhou. *In silico* toxicology prediction tools were applied to assess toxicity, enabling systematic exposure and health risk assessments, as well as the identification of priority contaminants for control. Total TDC concentrations ranged from 325 to 9,671 ng/g. 1,2-Diphenylguanidine (DPG) and 4-*N*-(4-methylpentan-2-yl)-1-*N*-phenylbenzene-1,4-diamine (6PPD) were the dominant compounds, accounting for 85% and 8.6% of the total concentration, respectively. The highest total concentration was observed in business districts (mean: 4,388 ng/g) and was correlated with traffic density. However, the notable concentrations detected in green spaces with low traffic volumes (mean: 847 ng/g) suggest that abrasion of other rubber materials during pedestrian activities may represent an additional source. Dry-season

¹SCNU Environmental Research Institute, Guangdong Provincial Key Laboratory of Chemical Pollution and Environmental Safety & MOE Key Laboratory of Theoretical Chemistry of Environment, South China Normal University, Guangzhou 510006, Guangdong, China.

²School of Environment, South China Normal University, Guangzhou 510006, Guangdong, China.

³Guangdong Provincial Engineering & Technology Research Center for Drinking Water Safety Assurance, School of Environment, South China Normal University, Guangzhou 510006, Guangdong, China.

Correspondence to: Prof. Jian-Liang Zhao, SCNU Environmental Research Institute, Guangdong Provincial Key Laboratory of Chemical Pollution and Environmental Safety & MOE Key Laboratory of Theoretical Chemistry of Environment, South China Normal University, Guangzhou 510006, Guangdong, China. E-mail: jianliang.zhao@m.scnu.edu.cn

concentrations were approximately twice those measured during the wet season, indicating that rainfall reduces TDC accumulation. Toxicity predictions identified neurotoxicity, carcinogenicity, mutagenicity, and endocrine disruption as the primary toxicological effects. Risk assessment indicated low health risks from inhalation and dermal contact, though attention is warranted. DPG, 6PPD, and 3H-1,3-benzothiazol-2-one were identified as priority pollutants requiring further monitoring. This study provides critical data to support future pollution control measures and regulatory strategies for TDCs in road dust.

INTRODUCTION

Tire-derived chemicals (TDCs) are collectively defined as compounds intentionally incorporated into tire products and road materials to improve product performance, including wear resistance, anticorrosion, and antioxidation, along with their environmentally formed transformation products^[1]. Since the journal *Science* reported in 2021 that 2,5-dianilino-cyclohexa-2,5-diene-1,4-dione (6PPD-Q) - a representative TDC - induces acute death in silver salmon in the Pacific Northwest at concentrations as low as the ng/L level, TDCs have emerged as pollutants of great concern^[2,3]. This concern has been further substantiated by a recent comprehensive review systematically elucidating the aquatic toxicity of 6PPD-Q^[4], underscoring the growing recognition of TDCs as priority emerging contaminants.

Based on the differences in chemical structure, TDCs are classified into four categories: *p*-phenylenediamines (PPDs), their quinone conversion products (PPD-quinones; PPD-Qs), benzothiazoles (BTs), and other TDCs^[5]. Compounds featuring a benzene ring disubstituted with amino groups (-NH₂) at the para positions are collectively referred to as PPDs, which are primarily incorporated into tire compounds as antioxidants. Their primary function is to extend the storage and service life of tires. Common PPDs include 4-*N*-(4-methylpentan-2-yl)-1-*N*-phenylbenzene-1,4-diamine (6PPD) and 2-(cyclohexylamino)-5-(phenylamino)cyclohexa-2,5-diene-1,4-dione (DTPD). As ozone oxidation products of PPDs, PPD-Qs mainly include 6PPD-Q and 2-anilino-5-(propan-2-ylamino)cyclohexa-2,5-diene-1,4-dione (IPPD-Q). These quinone derivatives generally exhibit higher toxicity than their parent compounds^[4]. BTs are a class of chemicals characterized by a rigid benzothiazole heterocyclic structure and primarily function as vulcanization accelerators (VAs) such as 1,3-benzothiazole (BTH) and 3H-1,3-benzothiazol-2-one (2-OH-BTH). They facilitate cross-linking reactions between tire polymers and vulcanizing agents (e.g., sulfur), thereby enhancing the physical properties and service life of tires. Compounds lacking distinct chemical structural features but widely used in tire products are defined as “other TDCs”, which mainly include 1,2-diphenylguanidine (DPG) and cross-linking agents such as hexa(methoxymethyl)melamine (HMMM). DPG has been widely detected in environmental matrices and is recognized as a major TDC^[6], while HMMM is primarily utilized in pre-coated metal sheets for white goods and architectural cladding, as well as in waterproof surface applications^[7,8]. Notably, several amine-based TDCs, including 6PPD and DPG, are listed as high-production-volume chemicals in the United States and Europe^[9].

Due to the absence of covalent bonding with the tire matrix, TDCs readily leach into the environment, resulting in widespread contamination. To date, various TDCs have been detected across multiple environmental matrices, including aquatic environments^[10], atmospheric particulates^[11], soil^[12], sediments^[13], and biota^[14]. Dust has long been recognized as both a reservoir and a major human exposure pathway for many environmental contaminants via ingestion, inhalation, and dermal contact^[15-17]. Therefore, it is very necessary to study the distribution of TDCs in dust. Previous studies have shown that TDCs are frequently detected in indoor dust. For instance, the typical TDCs 6PPD and DTPD have been detected in indoor dust, with concentrations ranging from 1.7 to 233 ng/g^[18,19]. Tan *et al.* further reported the occurrence of DPG and BTH in indoor dust, with median concentrations ranging from 5,030 to 11,400 ng/g and from 890 to

1,060 ng/g, respectively^[20]. In addition to indoor sources, TDC contamination in road dust has emerged as a significant environmental concern. Ginsberg *et al.* conducted a comprehensive survey of representative antioxidant-type TDCs in outdoor road dust^[21]. Their results revealed the widespread distribution of these antioxidants, with DPG and 6PPD-Q exhibiting the highest median concentrations of 121 and 9.75 ng/g, respectively. However, current research on TDCs in outdoor road dust remains limited, with studies mainly restricted to individual additive types, resulting in incomplete coverage of TDC species.

Furthermore, ubiquitous TDCs can enter organisms via dermal absorption, inhalation, and ingestion, eliciting diverse toxic effects such as metabolic toxicity, reproductive toxicity, and endocrine disruption. For instance, 6PPD-Q, which has gained widespread attention due to its association with acute coho salmon mortality, inhibits the activity of lipolysis-related enzymes and downregulates related gene expression, leading to abnormal lipid metabolism and metabolic toxicity^[22]. In addition, DPG, the most frequently detected TDC with the highest environmental concentrations, has been associated with allergic dermatitis^[23]. Furthermore, Dsikowitzky *et al.* identified potential genotoxicity associated with common processing accelerators such as HMMM^[24]. Emerging evidence also suggests that certain TDCs possess endocrine-disrupting potential. Chang *et al.* reported that 6PPD exhibited thyroid-disrupting activity, whereas its metabolite 6PPD-Q showed no such effects^[25]. These toxic TDCs can enter the human body through dust ingestion and dermal contact, posing potential health risks. Therefore, comprehensive toxicity prediction and health risk assessment of TDCs are imperative. However, current assessments of TDC toxicity primarily rely on traditional *in vivo* and *in vitro* assays. These methods are laborious, costly, and ethically challenging due to their reliance on animal testing, and they often focus on isolated toxicity endpoints. Consequently, there is a pressing need for more rapid and efficient strategies to enable comprehensive toxicity profiling and health risk assessment of TDCs.

The present study focused on Guangzhou, South China, which is characterized by the highest highway network density in the country and a substantial population of residents and motor vehicles. Specifically, this study aimed to: (1) investigate the occurrence, seasonal variation, and spatial distribution of 30 TDCs in road dust collected from four different functional areas; (2) predict the comprehensive toxicity profiles of these 30 TDCs using the *in silico* tool ProTox 3.0; and (3) assess human exposure risks associated with these TDCs and identify priority pollutants. This study shifts the focus toward TDCs in outdoor environments by broadening the spectrum of target analytes and employing an *in silico* tool to profile their potential toxicity. Combined with health risk assessment, this approach enables the identification of priority pollutants and provides critical data to inform future management strategies for TDCs in road dust.

MATERIALS AND METHODS

Chemicals and reagents

The selected 30 target TDCs, including 6 PPDs, 4 PPD-Qs, 12 BTs, and 8 other compounds, were chosen to represent the major chemical classes of tire additives and their transformation products based on their environmental relevance, toxicological concerns, and analytical feasibility. The 6 PPDs are 1-*N*,4-*N*-dinaphthalen-2-ylbenzene-1,4-diamine (DNPD), 6PPD, 1-*N*-cyclohexyl-4-*N*-phenylbenzene-1,4-diamine (DPPD), DTPD, 2-anilino-5-(4-methylpentan-2-ylamino)cyclohexa-2,5-diene-1,4-dione (CPPD), and 1-*N*,4-*N*-diphenylbenzene-1,4-diamine (IPPD). The 4 PPD-Qs included 6PPD-Q, 4-*N*-(2-methylphenyl)-1-*N*-(4-methylphenyl)benzene-1,4-diamine (CPPD-Q), 1-*N*-phenyl-4-*N*-propan-2-ylbenzene-1,4-diamine (DTPD-Q), and IPPD-Q. The 12 BTs are 2-methyl-1,3-benzothiazole (2-Me-BTH), 1,3-benzothiazol-2-amine (2-ABTH), 2-methylsulfanyl-1,3-benzothiazole (2-Me-S-BTH), 2-OH-BTH, BTH, 2H-benzotriazole (BT), *N*-(1,3-benzothiazol-2-ylsulfanyl)cyclohexanamine (CBS), *N*-(1,3-benzothiazol-2-ylsulfanyl)-*N*

-cyclohexylcyclohexanamine (DCBS), 4-(1,3-benzothiazol-2-ylsulfanyl)morpholine (NOBS), *N*-(1,3-benzothiazol-2-ylsulfanyl)-2-methylpropan-2-amine (TBBS), 2-(1,3-benzothiazol-2-ylsulfanyl)-1,3-benzothiazole (DM), and 9,9-dimethyl-10H-acridine (BLE). The remaining eight TDCs included 4-anilinophenol (4-HDPA), 1,3-dicyclohexylurea (DCU), 1,3-diphenylurea (DPU), HMMM, 2,2,4-trimethyl-1H-quinoline (RD), dimethylcarbamothioylsulfanyl *N,N*-dimethylcarbamodithioate (TMTD), DPG, and *N*-cyclohexyl-*N*-methylcyclohexanamine (DCA). During the experiments, three internal standards, namely 6PPD-quinone-d5, BT-d4, and Atrazine-d5, were used. These high-purity standards ($\geq 98\%$) were purchased from various vendors. The abbreviations, molecular formulas, Chemical Abstracts Service (CAS) registry numbers, chemical structures, and suppliers of the 30 target TDCs are summarized in [Supplementary Table 1](#). The organic reagents used in the experiments, such as methanol and dichloromethane, were high-performance liquid chromatography (HPLC) grade and purchased from Merck (Düsseldorf, Germany). Stock standard solutions of each target compound were prepared in methanol and subsequently stored at $-20\text{ }^{\circ}\text{C}$ until use.

Dust sample collection and pretreatment

According to the intensity of human activities, 12 sampling sites were selected in Guangzhou across four functional areas: business districts ($n = 4$), urban villages ($n = 2$), green spaces ($n = 3$), and residential areas ($n = 3$). Road dust samples were collected from these same sites in September 2022 (wet season) and March/April 2023 (dry season) using pre-cleaned brushes, resulting in a total of 24 samples. At each site, five subsamples were collected (one from the road centerline and four from surrounding positions) and mixed to generate one homogenate. All collected dust was wrapped in aluminum foil, sealed in polypropylene bags, transported to the laboratory, and stored at $-20\text{ }^{\circ}\text{C}$ pending chemical analysis. The selected areas and sampling points are shown in [Figure 1](#). Detailed information on each sampling event is provided in [Supplementary Table 2](#).

The dust extraction procedure was adapted from previously published methods with specific modifications^[26]. Briefly, approximately 100 mg of sieved dust (250 μm mesh) was weighed into a 30 mL glass centrifuge tube, and spiked with 100 ng of a mixture of three internal standards. The sample was ultrasonicated with 5 mL methanol for 30 min at room temperature, followed by a second extraction with 5 mL dichloromethane under ultrasonication for 30 min. After centrifugation (3,500 rpm, 5 min), the combined supernatants were collected, dried under a gentle nitrogen stream, and reconstituted in 1 mL methanol. Finally, the extracts were filtered through 0.22 μm nylon membranes (Anpu Co., Shanghai, China) prior to instrumental analysis.

Instrumental analysis

The target analytes and internal standards were analyzed using ultra-performance liquid chromatography coupled with a Xevo TQ-S triple quadrupole mass spectrometer (UPLC-ESI-MS/MS; Waters, Milford, MA, USA) equipped with an electrospray ionization (ESI) source. Chromatographic separation was performed on a Waters BEH C18 column (50 mm \times 2.1 mm, 1.7 μm) with an inline filter (2.1 mm, 0.2 μm) connected before the column to remove fine particles from the mobile phase and samples. The column temperature was maintained at $40\text{ }^{\circ}\text{C}$, and the injection volume was 5 μL . The mobile phase consisted of (A) 0.1% (v/v) formic acid in Milli-Q water and (B) methanol, at a flow rate of 0.3 mL/min. The gradient elution program was as follows: 0 min, 30% B; 1 min, 70% B; 1.5 min, 80% B; 2 min, 100% B; 4 min, 100% B; 5.5 min, 70% B; and 6.5 min, 70% B. The total run time was 5 min, with an additional 1.5 min for column re-equilibration before the next injection. All compounds were detected in positive electrospray ionization mode [ESI(+)] under multiple reaction monitoring (MRM). The ion source parameters were as follows: desolvation gas temperature, $500\text{ }^{\circ}\text{C}$; desolvation gas flow rate, 4 L/min; sheath gas temperature, $300\text{ }^{\circ}\text{C}$; sheath gas flow rate, 12 L/min; nozzle voltage, 500 V; capillary voltage, 2,500 V; and nebulizer pressure, 101 psi. The detailed mass

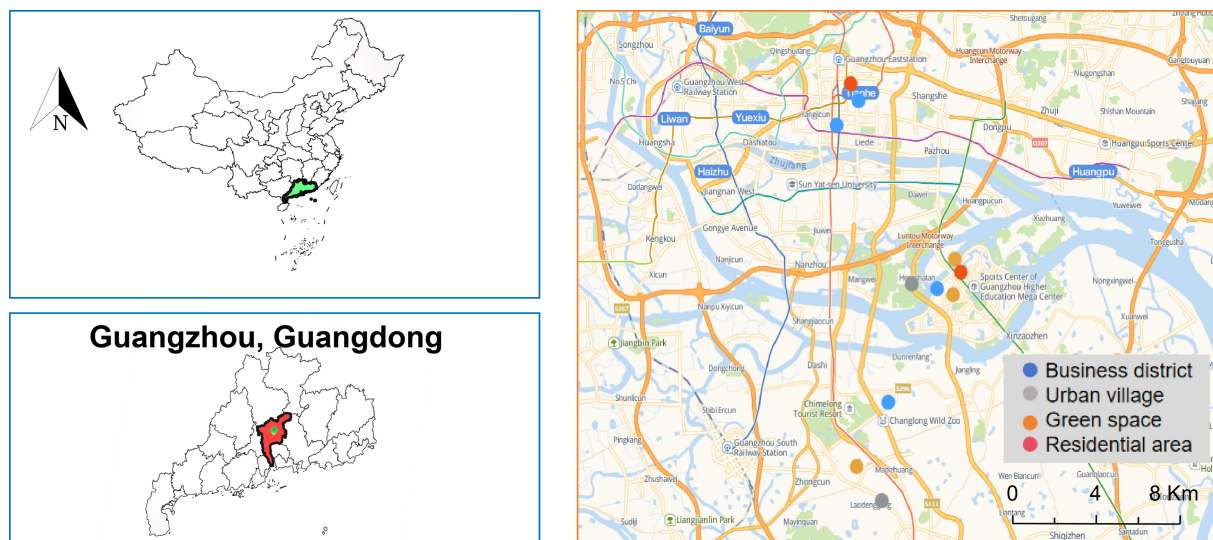


Figure 1. Map of sampling locations across different functional areas in Guangzhou. Basemap: © OpenStreetMap contributors.

spectrometry parameters, including MRM transitions and retention times of the target compounds, are listed in [Supplementary Tables 3 and 4](#).

Quality assurance and quality control

Comprehensive quality control measures were systematically implemented throughout the analytical process. Field blanks and procedural blanks were incorporated in each experimental batch to monitor potential background contamination. Additionally, solvent blanks and standard substances (100 µg/L for each target analyte) were analyzed to evaluate instrument performance. Matrix spike tests at 100 ppb were performed in triplicate to assess method accuracy, demonstrating recovery rates of 50%-124% for all 30 target compounds in road dust matrices [[Supplementary Table 5](#)]. The limits of detection (LODs) and limits of quantification (LOQs) for target pollutants in road dust were calculated using the signal-to-noise ratio approach, and analyte concentrations were determined via the internal standard method [[Supplementary Table 5](#)]. All data were blank-corrected by subtracting blank values from sample measurements. For all quantitative batches, the correlation coefficients (R^2) of the calibration curves (0.1-200 µg/L) exceeded 0.99.

In silico toxicity prediction tools and methods

This study utilized ProTox 3.0, a computational toxicology prediction tool, to assess the toxicity of 30 TDCs. ProTox 3.0 was selected due to its broad applicability and robust validation across diverse chemical classes, including emerging organic contaminants^[27]. The platform employs machine learning and computational chemistry methods to predict a variety of toxicological endpoints - such as acute and organ toxicity, carcinogenicity, mutagenicity, and endocrine disrupting potential - based solely on molecular structure. It integrates molecular similarity analysis, fragment-based toxicophore identification, and machine learning models to predict multiple toxicity endpoints with high accuracy and coverage. Its applicability domain encompasses a wide range of environmental pollutants, making it suitable for screening-level assessment of TDCs. Furthermore, the tool provides acute oral toxicity predictions and classifies compounds into toxicity classes according to the predicted median lethal dose (LD_{50}) as follows: Classes I & II (fatal if swallowed, $LD_{50} \leq 50$ mg/kg), Class III (toxic if swallowed, $50 < LD_{50} \leq 300$ mg/kg), Class IV (harmful if swallowed, $300 < LD_{50} \leq 2,000$ mg/kg), Class V (may be harmful if swallowed, $2,000 < LD_{50} \leq 5,000$ mg/kg), and Class VI (non-toxic, $LD_{50} > 5,000$ mg/kg).

Comprehensive toxicity predictions were performed for 30 TDCs across 11 toxicological endpoints, including hepatotoxicity, neurotoxicity, carcinogenicity, immunotoxicity, mutagenicity, cytotoxicity, and receptor-mediated toxicities [aryl hydrocarbon receptor (AhR), androgen receptor (AR), estrogen receptor alpha (ER α), and transthyretin (TTR)]. The selection of these endpoints was informed by existing knowledge of tire additive toxicology and concerns raised in previous studies regarding their potential adverse effects^[28]. The canonical Simplified Molecular Input Line Entry System (SMILES) notations of each compound were first retrieved from PubChem using their CAS registry numbers. These molecular structures were subsequently submitted to the ProTox 3.0 platform, where all specified toxicity endpoints were selected for prediction, generating corresponding toxicity profiles.

Data and statistical analysis

Instrumental data were processed using MassLynx software (v4.1, Waters Corp.). To correct for analyte loss during sample preparation, an internal standard method was employed; the corresponding internal standard for each target compound is detailed in [Supplementary Table 4](#). Each sample was analyzed in triplicate, and the mean concentration was used as the representative value. Statistical analyses were performed using SPSS Statistics (v27.0.1, IBM Corp.). Data normality was assessed using the Shapiro-Wilk test. For normally distributed data, parametric tests [independent-samples *t*-test, paired-samples *t*-test, one-way analysis of variance (ANOVA) followed by Tukey's post hoc test] were applied, whereas non-normally distributed data were analyzed using non-parametric tests (Mann-Whitney *U* test and Kruskal-Wallis test). Spearman's rank correlation analysis was performed to evaluate inter-compound correlations. Statistical significance was defined as $P < 0.05$. Relevant figures were generated using Origin (2021, OriginLab Corp.).

Human exposure assessment and health risk

This study employed the estimated daily intake (EDI) metric to assess non-dietary exposure risks to TDCs through incidental dust ingestion and dermal contact. The EDI (ng/kg bw/day) was calculated as follows:

$$EDI = EDI_{\text{ingestion}} + EDI_{\text{dermal}} \quad (1)$$

$$EDI_{\text{ingestion}} = \frac{C \times EF \times IGR}{BW} \quad (2)$$

$$EDI_{\text{dermal}} = \frac{C \times SA \times AF \times ABS \times EF}{BW} \quad (3)$$

Based on exposure assessment frameworks recommended by the U.S. Environmental Protection Agency (EPA)^[29,30] and Wang *et al.*^[31], EDI represents the sum of oral dust ingestion ($EDI_{\text{ingestion}}$) and dermal contact (EDI_{dermal}). *C* is the mean concentration of target analytes in road dust (ng/g). *EF* is the exposure frequency (days/year); *IGR* is the dust ingestion rate (mg/day); *BW* is the human body weight (kg); *SA* is the skin surface area available for contact (cm²/day); *AF* is the dust-to-skin adherence factor (mg/cm²); and *ABS* is the dermal absorption factor (unitless). All parameters were adopted from Jin *et al.* and are summarized in [Supplementary Table 6](#)^[32].

To further evaluate human health risks associated with the 30 TDCs and prioritize compounds, predicted Lethal Dose 50 (LD_{50}) values were converted to reference doses (RfDs) using Equation (4)^[21]. The hazard quotient (HQ) was subsequently calculated as the ratio of EDI to RfD^[33], as defined below:

$$RfD = \frac{LD_{50}}{1000} \quad (4)$$

$$HQ = \frac{EDI}{RfD} \quad (5)$$

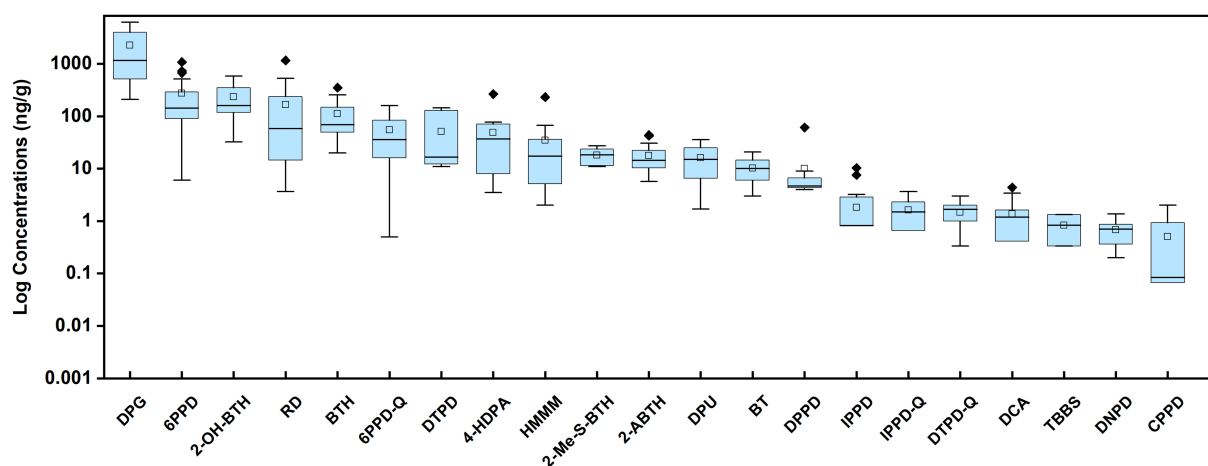


Figure 2. Concentration distribution of widely detected TDCs in road dust ($n = 24$ for each compound). The box represents the IQR from the 25th to the 75th percentile; the black line inside the box denotes the median; the open square (\square) indicates the mean; and diamond symbols (\blacklozenge) represent outliers (extending to the minimum and maximum values within $1.5 \times$ IQR). TDCs: Tire-derived chemicals; IQR: interquartile range; DPG: 1,2-diphenylguanidine; 6PPD: 4-*N*-(4-methylpentan-2-yl)-1-*N*-phenylbenzene-1,4-diamine; 2-OH-BTH: 3H-1,3-benzothiazol-2-one; RD: 2,2,4-trimethyl-1H-quinoline; BTH: 1,3-benzothiazole; 6PPD-Q: 2,5-dianilino-cyclohexa-2,5-diene-1,4-dione; DTPD: 2-(cyclohexylamino)-5-(phenylamino)cyclohexa-2,5-diene-1,4-dione; 4-HDPA: 4-anilinophenol; HMMM: hexa(methoxymethyl)melamine; 2-Me-S-BTH: 2-methylsulfanyl-1,3-benzothiazole; 2-ABTH: 1,3-benzothiazol-2-amine; DPU: 1,3-diphenylurea; BT: 2H-benzotriazole; DPPD: 1-*N*-cyclohexyl-4-*N*-phenylbenzene-1,4-diamine; IPPD: 1-*N*,4-*N*-diphenylbenzene-1,4-diamine; IPPD-Q: 2-anilino-5-(propan-2-ylamino)cyclohexa-2,5-diene-1,4-dione; DTPD-Q: 1-*N*-phenyl-4-*N*-propan-2-ylbenzene-1,4-diamine; DCA: *N*-cyclohexyl-*N*-methylcyclohexanamine; TBBS: *N*-(1,3-benzothiazol-2-ylsulfanyl)-2-methylpropan-2-amine; DNPD: 1-*N*,4-*N*-dinaphthalen-2-ylbenzene-1,4-diamine; CPPD: 2-anilino-5-(4-methylpentan-2-ylamino)cyclohexa-2,5-diene-1,4-dione.

RESULTS AND DISCUSSION

Occurrence of TDCs in road dust

The concentration distribution of TDCs in road dust from various functional areas is illustrated in [Figure 2](#). Detailed information on detection frequency (DF), median, mean concentrations, and concentration ranges of the 6 PPDs, 4 PPD-Qs, 12 BTs, and 8 other TDCs is provided in [Supplementary Table 7](#). As shown in [Figure 2](#), [Supplementary Figure 1A](#) and [Supplementary Table 7](#), the total concentrations of the 30 TDCs in road dust ranged from 325 to 9,671 ng/g. Notably, DPG, 6PPD, 6PPD-Q, and HMMM were detected in all functional areas, indicating their widespread presence in road dust, which aligns with the findings of Liu *et al.*^[34]. This finding is further supported by Breider *et al.*^[35], who reported that DPG (18%) and 6PPD (15%) were among the most frequently detected tire-derived compounds in vegetables from Swiss markets, confirming the ubiquitous presence of these chemicals across different environmental media. Our study also presents new insights. In particular, 4-HDPA and DPU - transformation products of DPPD^[36] and DPG, respectively - were detected across all functional areas, with mean concentrations of 48.6 and 16.1 ng/g, respectively. This underscores the importance of monitoring not only parent TDCs in road dust but also their transformation products. In contrast, CPPD-Q, 2-Me-BTH, NOBS, DCU, BLE, and DM were not detected in any of the samples, suggesting either very low environmental concentrations or effective elimination during industrial processes.

[Supplementary Figure 1B](#) depicts the concentration distribution of four TDC categories (PPDs, PPD-Qs, BTs, and others). PPDs exhibited significantly higher concentrations than BYs in road dust (123 vs. 69 ng/g; one-way ANOVA with Tukey's post hoc test, $P < 0.05$). This difference is likely due to the higher lipophilicity of PPDs (log Kow: 4.0-6.0) compared to BTs (log Kow: 2.0-3.0), suggesting that physicochemical properties influence the environmental distribution of TDCs, with more lipophilic compounds tending to accumulate in road dust. Previous studies have reported higher concentrations of PPD-Qs relative to their parent PPDs in aquatic environments due to oxidation and biodegradation processes^[37,38]. However, in this study, substantially lower concentrations of PPD-Qs compared to PPDs were found in road dust samples. This suggests that oxidation and biodegradation processes are less pronounced in dust matrices than in aquatic

systems, thereby limiting the transformation of PPDs to PPD-Qs.

Among the 6 PPDs analyzed, 6PPD was detected in all functional areas and exhibited the highest concentrations (ranging from 6 to 1,082 ng/g, with a median of 130 ng/g), accounting for 8.6% of the total TDC concentration (based on the ratio of the mean concentration of 6PPD to the mean concentration of the 30 TDCs across all samples) [Figure 3 and Supplementary Table 7]. This predominance of 6PPD may be attributed to its substantial global production volume (e.g., 22,700-45,400 tons in the United States^[39]; 10,000-100,000 tons in Europe^[40]). In this study, the median concentration of 6PPD in road dust (130 ng/g) was comparable to levels reported in Australian dust samples (median: 101 ng/g) but lower than those reported in Japan (range: 323-356 ng/g)^[41]. We hypothesize that these geographical differences may be influenced by varying traffic densities across countries, given that TDCs are primarily incorporated into automotive tires and road materials. Furthermore, comparison with indoor dust data from Huang *et al.* revealed a substantially lower median concentration of 6PPD in indoor environments (14 ng/g) than in our road dust samples (130 ng/g)^[18]. This pronounced contrast further supports the likelihood of outdoor, vehicle-related sources as the dominant origin of 6PPD in the environment.

Among the four PPD-Qs analyzed, 6PPD-Q was detected in all functional areas and exhibited the highest concentrations, ranging from 0.50 to 159 ng/g (DF: 100%) [Figure 3 and Supplementary Table 7]. Meanwhile, Huang *et al.* reported median concentrations of 6PPD-Q in road dust (32.2 ng/g), which are comparable to those observed in our investigation (38.8 ng/g)^[18]. The high environmental prevalence of 6PPD-Q may partially result from the ozone-driven oxidation of its parent compound, 6PPD^[42]. DTPD-Q and IPPD-Q were also frequently detected in road dust (DF > 60%), indicating their widespread occurrence in roadway matrices, consistent with prior research^[43]. Notably, CPPD-Q was not detected in any samples. This absence may be attributed to factors such as lower production volumes, limited usage in tire formulations, or differences in environmental persistence and transformation pathways, requiring further investigation.

For BTs, the two most prominent compounds were 2-OH-BTH and BTH, with concentration ranges of ND-607 ng/g and ND-351 ng/g, respectively [Figure 3 and Supplementary Table 7]. This prevalence likely results from the widespread addition of BTH to tires for rubber vulcanization, enhancing mechanical strength and wear resistance^[44,45]. As tires abrade on road surfaces, significant amounts of BTH are released into road dust. Furthermore, BTH can undergo oxidation to form 2-OH-BTH^[46], contributing to the co-occurrence of both compounds in road dust. Except for 2-Me-BTH and NOBS, which were not detected in any samples, other BTs were quantifiable. The median concentrations of 2-ABTH, 2-Me-S-BTH, and BT were 14.3, 18.3, and 10.0 ng/g, respectively. In contrast, notably lower mean concentrations (< 3 ng/g) were observed for CBS, DCBS, and TBBS.

Among other tire additives, DPG, a VA used in rubber products such as tires, furniture, and shoes^[47], exhibited the highest concentrations, ranging from 208 to 7,661 ng/g, accounting for 85% of the total TDC concentration (based on the ratio of the mean concentration of DPG to the mean concentration of the 30 TDCs across all samples) [Figure 3 and Supplementary Table 7]. However, Tan *et al.* investigated DPG in indoor dust and reported concentrations ranging from 5,030 to 11,400 ng/g, which are notably higher (by approximately one order of magnitude) than those in our road dust samples^[20]. This substantial discrepancy may be attributed to the widespread incorporation of DPG into indoor furnishings, toys, and gloves, suggesting a greater prevalence of indoor sources. Additionally, four other substances - 4-HDPA, DPU, HMMM, and RD - were ubiquitously detected in road dust (DF > 80%), but their concentrations were substantially lower (ND-1,156 ng/g) compared to DPG. This difference may reflect lower usage volumes and/or reduced environmental release despite their presence in tire formulations. Notably, DCU was not detected in any samples, potentially indicating its phase-out or minimal use in contemporary tire formulations.

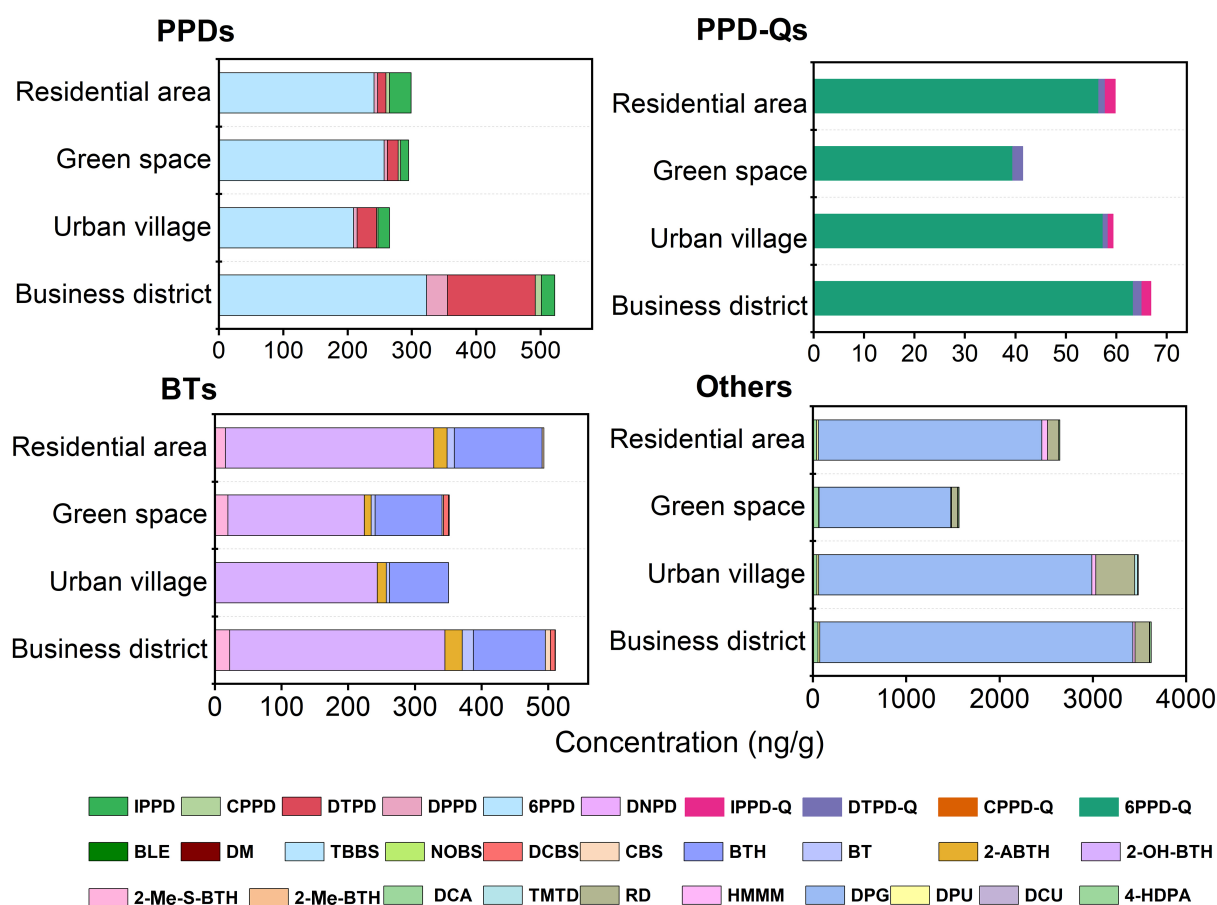


Figure 3. Mean concentration of 30 TDCs in road dust from various functional areas. Error bars are omitted for clarity; concentration ranges for each compound are available in [Supplementary Table 7](#). TDCs: Tire-derived chemicals; PPDs: p-phenylenediamines; PPD-Qs: quinone conversion products of p-phenylenediamines; BTs: benzothiazoles; Others: other TDCs; IPPD: 1-N,4-N-diphenylbenzene-1,4-diamine; CPPD: 2-anilino-5-(4-methylpentan-2-ylamino)cyclohexa-2,5-diene-1,4-dione; DTPD: 2-(cyclohexylamino)-5-(phenylamino)cyclohexa-2,5-diene-1,4-dione; DPPD: 1-N-cyclohexyl-4-N-phenylbenzene-1,4-diamine; 6PPD: 4-N-(4-methylpentan-2-yl)-1-N-phenylbenzene-1,4-diamine; DNPB: 1-N,4-N-dinaphthalen-2-ylbenzene-1,4-diamine; IPPD-Q: 1-N-phenyl-4-N-propan-2-ylbenzene-1,4-diamine; DTPD-Q: 2,5-dianilino-cyclohexa-2,5-diene-1,4-dione; 6PPD-Q: 2,5-dianilino-cyclohexa-2,5-diene-1,4-dione; BLE: 9,9-dimethyl-10H-acridine; DM: 2-(1,3-benzothiazol-2-yl)disulfanyl-1,3-benzothiazole; TBBS: N-(1,3-benzothiazol-2-ylsulfanyl)-2-methylpropan-2-amine; NOBS: 4-(1,3-benzothiazol-2-ylsulfanyl)morpholine; DCBS: N-(1,3-benzothiazol-2-ylsulfanyl)-N-cyclohexylcyclohexanamine; CBS: N-(1,3-benzothiazol-2-ylsulfanyl)cyclohexanamine; BTH: 1,3-benzothiazole; BT: 2H-benzotriazole; 2-ABTH: 1,3-benzothiazol-2-amine; 2-OH-BTH: 3H-1,3-benzothiazol-2-one; 2-Me-S-BTH: 2-methylsulfanyl-1,3-benzothiazole; 2-Me-BTH: 2-methyl-1,3-benzothiazole; DCA: N-cyclohexyl-N-methylcyclohexanamine; TMTD: dimethylcarbamothioylsulfanyl N,N-dimethylcarbamodithioate; RD: 2,2,4-trimethyl-1H-quinoline; HMMM: hexa(methoxymethyl)melamine; DPG: 1,2-diphenylguanidine; DPU: 1,3-diphenylurea; DCU: 1,3-dicyclohexylurea; 4-HDPA: 4-anilinophenol.

Correlation analysis of the 24 detected TDCs (excluding six substances not detected at any sampling points: BLE, DM, DCU, NOBS, 2-Me-BTH, and CPPD-Q) in road dust across functional areas is presented in [Supplementary Figure 2](#). Overall, significant positive correlations ($r = 0.6-0.9$, $P < 0.05$) were observed among most TDCs, suggesting common sources. Notably, strong correlations ($r > 0.9$) were found between parent compounds (BTs and PPDs) and their respective transformation products. These results indicate that the levels of transformation products in road dust are linked to the environmental transformation of their parent chemicals. Therefore, the distribution of TDCs in road dust is strongly influenced not only by their physicochemical properties, sources, and usage patterns, but also, more significantly, by traffic density.

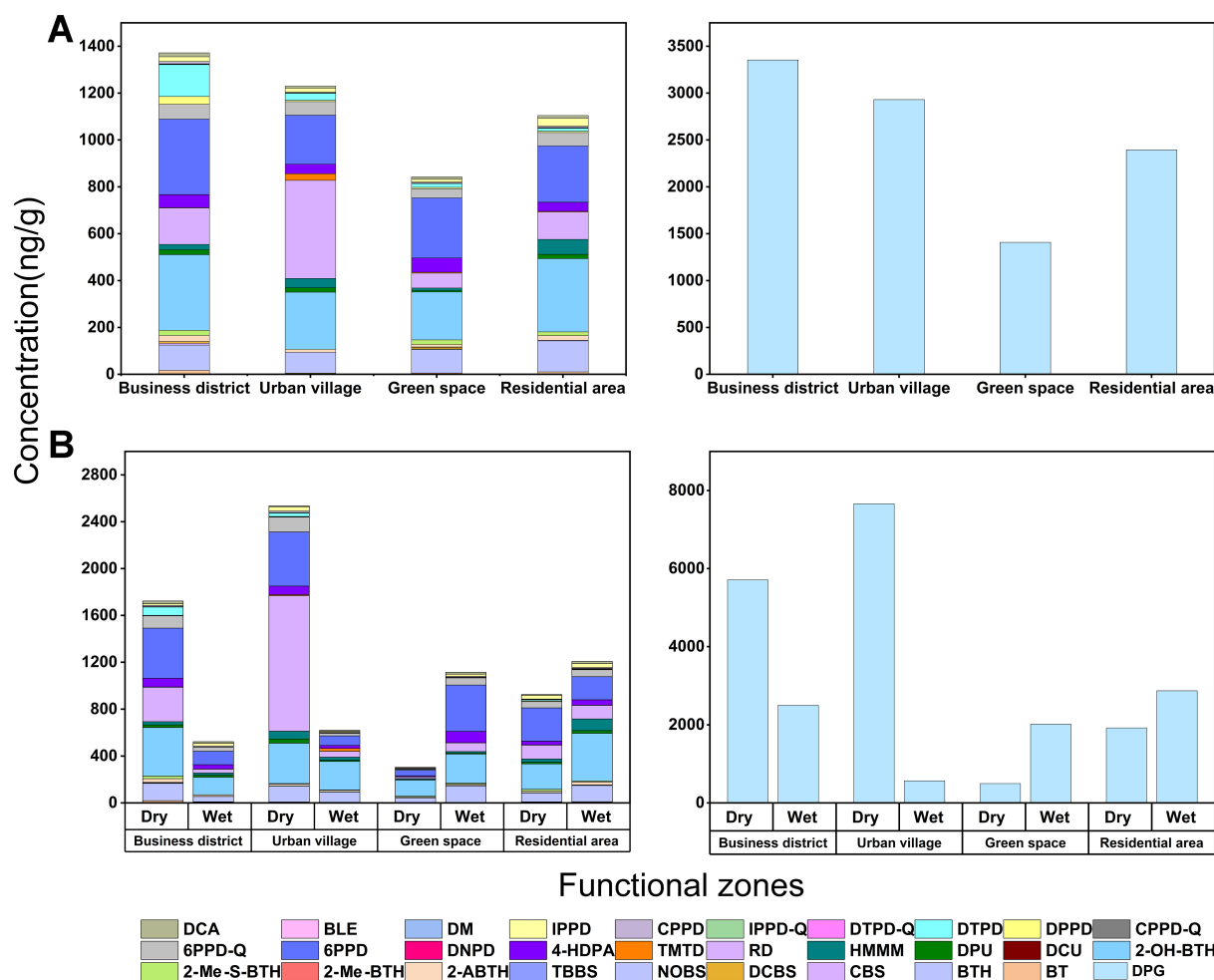


Figure 4. (A) Spatial variations of 30 TDCs in road dust; (B) Seasonal variations of 30 TDCs. The right panel presents the spatial and seasonal distribution of DPG separately. TDCs: Tire-derived chemicals; DPG: 1,2-diphenylguanidine; DCA: *N*-cyclohexyl-*N*-methylcyclohexanamine; BLE: 9,9-dimethyl-10H-acridine; DM: 2-(1,3-benzothiazol-2-yl)disulfanyl-1,3-benzothiazole; IPPD: 1-*N*,4-*N*-diphenylbenzene-1,4-diamine; CPPD: 2-anilino-5-(4-methylpentan-2-ylamino)cyclohexa-2,5-diene-1,4-dione; IPPD-Q: 2-anilino-5-(propan-2-ylamino)cyclohexa-2,5-diene-1,4-dione; DTPD-Q: 1-*N*-phenyl-4-*N*-propan-2-ylbenzene-1,4-diamine; DTPD: 2-(cyclohexylamino)-5-(phenylamino)cyclohexa-2,5-diene-1,4-dione; DPPD: 1-*N*-cyclohexyl-4-*N*-phenylbenzene-1,4-diamine; CPPD-Q: 4-*N*-(2-methylphenyl)-1-*N*-(4-methylphenyl)benzene-1,4-diamine; 6PPD-Q: 2,5-dianilino-cyclohexa-2,5-diene-1,4-dione; 6PPD: 4-*N*-(4-methylpentan-2-yl)-1-*N*-phenylbenzene-1,4-diamine; DNPD: 1-*N*,4-*N*-dinaphthalen-2-ylbenzene-1,4-diamine; 4-HDPA: 4-anilinophenol; TMTD: dimethylcarbamothioylsulfanyl *N,N*-dimethylcarbamodithioate; RD: 2,2,4-trimethyl-1H-quinoline; HMMM: hexa(methoxymethyl)melamine; DPU: 1,3-diphenylurea; DCU: 1,3-dicyclohexylurea; 2-OH-BTH: 3H-1,3-benzothiazol-2-one; 2-Me-S-BTH: 2-methylsulfanyl-1,3-benzothiazole; 2-Me-BTH: 2-methyl-1,3-benzothiazole; 2-ABTH: 1,3-benzothiazol-2-amine; TBBS: *N*-(1,3-benzothiazol-2-ylsulfanyl)-2-methylpropan-2-amine; NOBS: 4-(1,3-benzothiazol-2-ylsulfanyl)morpholine; DCBS: *N*-(1,3-benzothiazol-2-ylsulfanyl)-*N*-cyclohexylcyclohexanamine; CBS: *N*-(1,3-benzothiazol-2-ylsulfanyl)cyclohexanamine; BTH: 1,3-benzothiazole; BT: 2H-benzothiazole.

Spatial and seasonal variations of TDCs in road dust

Figure 4A presents the total concentrations of the 30 TDCs across different functional areas. The contamination levels followed the order: business district > urban village > residential area > green space. Overall, the highest total concentration was observed in business districts (mean: 4,388 ng/g), likely due to their denser traffic flow. Notably, TDCs were also detected in green spaces (characterized by high pedestrian activity but low vehicle traffic), albeit at lower total concentrations (mean: 847 ng/g). This finding suggests that tire wear from rubber abrasion on shoe soles and atmospheric transport may also contribute to TDC contamination in green spaces^[48,49]. Furthermore, substantial concentrations of TDCs were also detected in residential areas and urban villages, which may be attributed to human activities and the low street-sweeping frequency^[50].

Concurrently, we analyzed the compositional profiles of TDCs across different functional zones, as shown in [Figure 4A](#). Overall, no significant differences were observed in the compositional distribution of TDCs among these functional zones. Human and vehicular traffic intensity primarily influenced the total concentrations of TDCs rather than their compositional patterns. This suggests that the sources and release mechanisms of the various TDCs are consistent across all zones.

[Figure 4B](#) presents the seasonal variations of the 30 target TDCs in road dust across different functional areas. Overall, the total concentrations of the 30 TDCs were significantly higher during the dry season (range: 672–9,671 ng/g) than during the wet season (range: 325–5,803 ng/g) (paired-samples *t*-test, $P < 0.05$). This disparity may be attributed to limited rainfall during the dry season, which facilitates the accumulation of TDCs in road dust. Conversely, rainfall events can transport TDCs into aquatic systems, thereby exacerbating water pollution and posing a threat to aquatic ecosystems^[51]. However, an opposite trend was observed in residential areas and green areas, where TDCs exhibited distinct seasonal patterns. This phenomenon may be associated with three key factors. First, local regulations and sanitation practices may play a role. Second, seasonal differences in tire wear rates could contribute; for instance, Rodovalho and de Tomi reported increased tire rolling resistance during the rainy season^[52]. Consequently, tire wear rates are higher during the rainy season compared to the dry season, potentially leading to elevated TDC concentrations in road dust during wet periods. Furthermore, the number of antecedent dry days also represents a significant influencing factor.

As depicted in [Figure 4B](#) and [Supplementary Figure 3](#), the compositional distribution of various TDCs remained consistent across seasons. This indicates that seasonal variation primarily affects the overall concentration of TDCs in road dust, while having a negligible effect on their compositional profiles. Consequently, it can be inferred that the sources of TDCs in road dust might remain stable across different seasons.

Predicted human toxicity

The acute toxicity, organ toxicity, toxicological endpoints, and toxicological pathways of the TDCs were predicted using ProTox 3.0, with “+” for positive/toxic effects and “-” for negative/nontoxic effects [[Supplementary Table 8](#)]. The prediction results showed that all the studied TDCs were within the applicability domain, indicating that the predictions were reliable.

As shown in [Figure 5A](#), the LD_{50} values of the 30 representative TDCs ranged from 215 to 7,000 mg/kg. Among them, IPPD-Q, DTPD-Q, DPPD, and 6PPD, with LD_{50} values of 215, 215, 244, and 271 mg/kg, respectively, were classified as Class III acute toxicity substances. This classification indicates that these substances exhibit high toxicity and may lead to various adverse toxicological effects. Consequently, future studies should prioritize investigating the environmental occurrence and health impacts of these four high-priority compounds. Moreover, the acute toxicity assessment indicated that quinone transformation products derived from PPD-derived antioxidants exhibit greater toxicity compared to their parent compounds, consistent with previous studies^[2]. As shown in [Supplementary Table 8](#), 23 of the 30 TDCs were found to exhibit neurotoxic effects, aligning with the findings reported by Ricarte *et al.*^[53]. Additionally, BTs demonstrated both neurotoxic and hepatotoxic effects. These results indicate that neurotoxicity is a primary concern for TDCs, and that the hepatotoxicity associated with BTs warrants further investigation.

In silico toxicity predictions identified carcinogenicity and mutagenicity as the primary toxicity endpoints for the TDCs. The binding interactions between the TDCs and specific receptors were evaluated to predict their toxicity potential mediated by the disruption of biological pathways. Among the four receptors examined, the TDCs demonstrated strong binding affinity for AhR and TTR, but only weak affinity for AR and ER^[25].

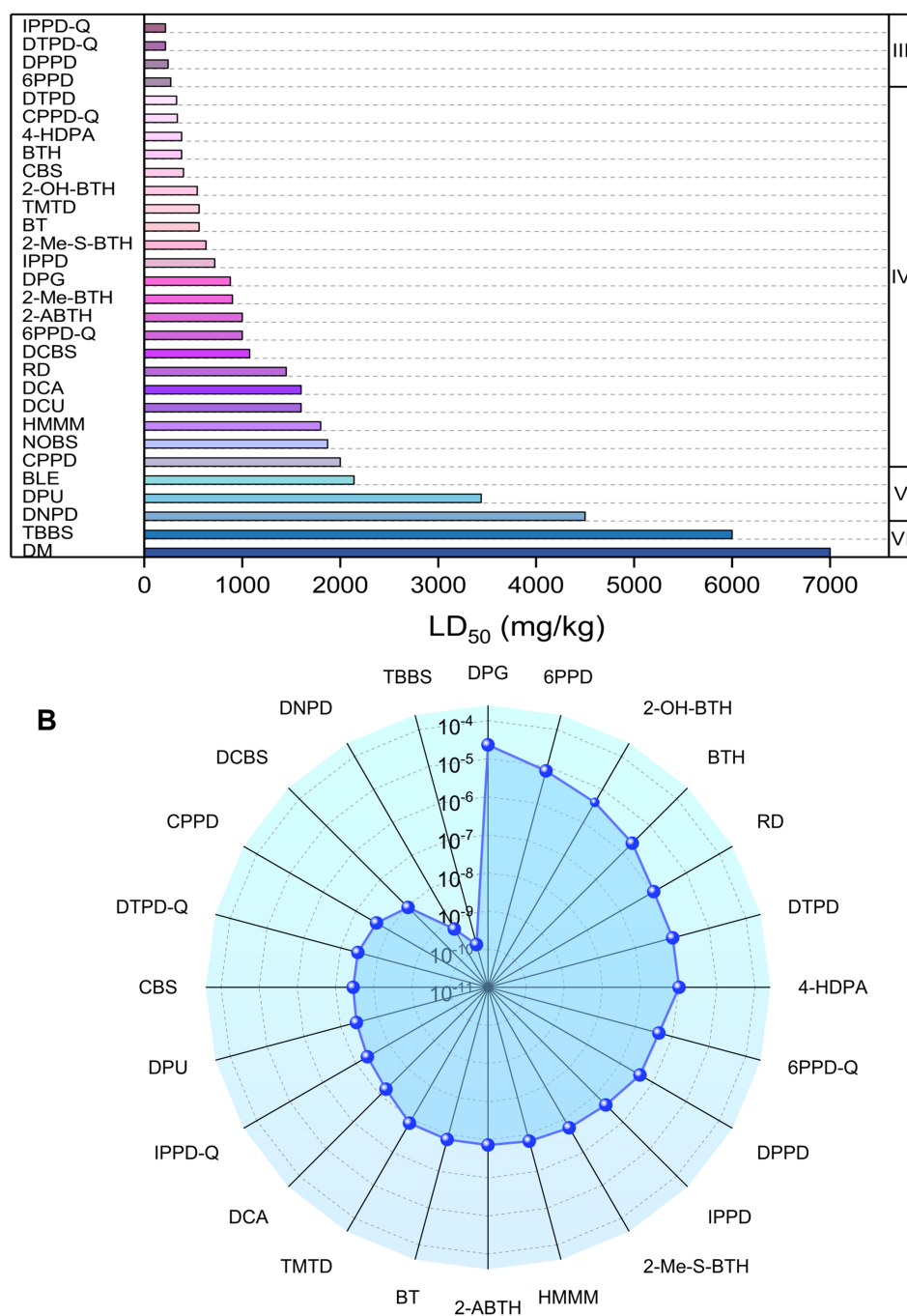


Figure 5. (A) Predicted median lethal dose (LD_{50}) values of 30 TDCs; (B) Distribution of HQ values for 24 TDCs. Six substances (CPPD-Q, 2-Me-BTH, NOBS, DCU, BLE, and DM) were excluded as they were not detected at any sampling site. TDCs: Tire-derived chemicals; HQ: hazard quotient; CPPD-Q: 4-*N*-(2-methylphenyl)-1-*N*-(4-methylphenyl)benzene-1,4-diamine; 2-Me-BTH: 2-methyl-1,3-benzothiazole; NOBS: 4-(1,3-benzothiazol-2-ylsulfanyl)morpholine; DCU: 1,3-dicyclohexylurea; BLE: 9,9-dimethyl-10H-acridine; DM: 2-(1,3-benzothiazol-2-ylsulfanyl)-1,3-benzothiazole; IPPD-Q: 2-anilino-5-(propan-2-ylamino)cyclohexa-2,5-diene-1,4-dione; DTPD-Q: 1-*N*-phenyl-4-*N*-propan-2-ylbenzene-1,4-diamine; DPPD: 1-*N*-cyclohexyl-4-*N*-phenylbenzene-1,4-diamine; 6PPD: 4-*N*-(4-methylpentan-2-yl)-1-*N*-phenylbenzene-1,4-diamine; DTPD: 2-(cyclohexylamino)-5-(phenylamino)cyclohexa-2,5-diene-1,4-dione; 4-HDPA: 4-anilinophenol; BTH: 1,3-benzothiazole; CBS: *N*-(1,3-benzothiazol-2-ylsulfanyl)cyclohexanamine; 2-OH-BTH: 3H-1,3-benzothiazol-2-one; TMTD: dimethylcarbamothioylsulfanyl *N,N*-dimethylcarbamodithioate; BT: 2H-benzotriazole; 2-Me-S-BTH: 2-methylsulfanyl-1,3-benzothiazole; IPPD: 1-*N*,4-*N*-diphenylbenzene-1,4-diamine; DPG: 1,2-diphenylguanidine; 2-ABTH: 1,3-benzothiazol-2-amine; 6PPD-Q: 2,5-dianilino-cyclohexa-2,5-diene-1,4-dione; DCBS: *N*-(1,3-benzothiazol-2-ylsulfanyl)-*N*-cyclohexylcyclohexanamine; RD: 2,2,4-trimethyl-1H-quinoline; DCA: *N*-cyclohexyl-*N*-methylcyclohexanamine; DCU: 1,3-dicyclohexylurea; HMMM: hexa(methoxymethyl)melamine; NOBS: 4-(1,3-benzothiazol-2-ylsulfanyl)morpholine; CPPD: 2-anilino-5-(4-methylpentan-2-ylamino)cyclohexa-2,5-diene-1,4-dione; BLE: 9,9-dimethyl-10H-acridine; DPU: 1,3-diphenylurea; DNPD: 1-*N*,4-*N*-dinaphthalen-2-ylbenzene-1,4-diamine; TBBS: *N*-(1,3-benzothiazol-2-ylsulfanyl)-2-methylpropan-2-amine; DM: 2-(1,3-benzothiazol-2-ylsulfanyl)-1,3-benzothiazole.

These findings suggest that such additives may induce AhR-mediated toxic responses and disrupt thyroid hormone function, while their estrogenic or androgenic toxicity is expected to be low. This concern is further supported by recent *in vivo* evidence demonstrating that 6PPD-Q exhibits tissue-specific bioaccumulation and hepatotoxicity in zebrafish, with toxicological mechanisms distinct from those of its parent compound 6PPD^[54]. The transformation products exhibited higher binding affinity for TTR, suggesting that environmental transformation may increase their potential to disrupt thyroid hormone homeostasis relative to their parent compounds.

Therefore, the toxicity predictions indicated that the primary toxic effects of the TDCs include neurotoxicity, carcinogenicity, mutagenicity, and thyroid hormone disruption. Furthermore, the toxic effects of transformation products warrant greater attention compared with those of their parent compounds. It should be noted that these predictions are exploratory in nature and based solely on molecular structures; therefore, they may not fully capture complex biological processes such as metabolism or mixture effects. Consequently, experimental validation (e.g., *in vitro* assays) is warranted to confirm these findings.

Human exposure implications and risk prioritization

Supplementary Table 9 summarizes the EDIs of 30 TDCs for children and adults via dust ingestion and dermal absorption across different functional areas. As shown in Supplementary Table 9 and Supplementary Figure 4, for both adults or children, the highest EDI was observed in the business district [mean \pm standard error (SE): 9.49 ± 2.70 and 65.4 ± 18.3 ng/(kg·d), respectively], followed by the urban village [8.44 ± 0.63 and 57.5 ± 4.30 ng/(kg·d)], the residential area [7.06 ± 1.96 and 47.5 ± 13.4 ng/(kg·d)], and the green space [4.52 ± 0.93 and 31.0 ± 6.3 ng/(kg·d)]. This spatial pattern corresponds to the total concentrations of TDCs in these areas. Overall, the EDI via dust exposure for adults was lower than that for children, indicating the greater sensitivity and vulnerability of children to these additives. DPG was the primary contributor to total intake, accounting for 61%–72% of exposure, suggesting its significant potential to enter the human body via dust and pose health risks, thereby warranting exposure control measures. This finding aligns with a recent study by Sherman *et al.*, which investigated tire-derived compounds in leafy vegetables and identified DPG as one of the most frequently detected compounds (21.4% of samples), with EDIs ranging from 0.05 to 4.0 ng/person/day^[55]. These results demonstrate that DPG not only dominates dust exposure but also represents a key contaminant in the food chain, further underscoring the need for comprehensive exposure management strategies across multiple pathways. While 6PPD-Q exhibited relatively low EDI contributions (1.3%–1.8%), its potential early-life health effects necessitate increased biomonitoring efforts^[56], particularly in children.

Concurrently, we conducted a health risk assessment and established a priority ranking for the 30 TDCs, as summarized in Figure 5B and Supplementary Table 10. The results demonstrated that the estimated intake of TDCs via dust ingestion was consistently at least four orders of magnitude lower than the predicted RfDs for the respective compounds. All calculated HQ values were below 1, indicating a relatively low health risk associated with exposure to these TDCs through dust. DPG, 6PPD, 2-OH-BTH, BTH, RD, DTPD, 4-HDPA, 6PPD-Q, and DPPD were identified as the top nine priority contaminants. Notably, two substances with high predicted toxicity - IPPD and DTPD-Q - were assigned lower priority rankings due to their low environmental concentrations. This finding underscores that health risk assessments of contaminants should consider not only intrinsic toxicity but also, more critically, environmental exposure levels. Overall, the health risk posed to humans by TDCs via dust exposure was low. However, this does not preclude the need for their management. It is crucial to note that our exposure assessment, which considered only dust ingestion and dermal contact and relied on estimated toxicity data, may have underestimated the cumulative exposure. These limitations introduce uncertainty into our conclusions.

CONCLUSIONS

This study systematically investigated the occurrence, spatial distribution, and potential health risks of 30 TDCs in road dust from Guangzhou. DPG and 6PPD were identified as the predominant TDCs, and their concentrations were correlated with population density and traffic volume. Seasonal analysis revealed that prolonged dry conditions promoted TDC accumulation in road dust. Based on integrated toxicity prediction and health risk assessment, DPG, 6PPD, and 2-OH-BTH were identified as priority pollutants, and children were found to face relatively higher exposure risks. These findings underscore the need for future studies to evaluate multiple exposure pathways and obtain comprehensive toxicological data to refine risk assessments of TDCs in urban environments.

DECLARATIONS

Authors' contributions

Methodology: Hu, R.; Liu, Y. H.; Liang, X. N.; Zhang, H. Y.; Huang, Z.; Li, Z. T.

Data analysis: Hu, R.; Liu, Y. H.

Sampling: Hu, R.; Lin, L. Q.

Study design, review and editing: Zhao, J. L.; Ying, G. G.; Hu, R.

All authors approved the final manuscript.

Availability of data and materials

The supplementary data associated with this article can be found in the [Supplementary Materials](#). Further data are available from the corresponding author upon reasonable request.

AI and AI-assisted tools statement

Not applicable.

Financial support and sponsorship

The authors acknowledge financial support from the National Natural Science Foundation of China (No. U21A2036), the Natural Science Foundation of Guangdong Province, China (No. 2024A1515011195), and the Guangdong Special Support Program (No. 2024TX08A357).

Conflicts of interest

Zhao, J. L. and Ying, G. G. are Editorial Board Members of *Journal of Environmental Exposure Assessment*. They were not involved in any stage of the editorial process, notably including reviewer selection, manuscript handling, or decision making. The other authors declared that there are no conflicts of interest.

Ethical approval and consent to participate

Not applicable.

Consent for publication

Not applicable.

Copyright

© The Author(s) 2026.

Supplementary Materials

[Supplementary Materials](#)

REFERENCES

1. Baensch-Baltruschat, B.; Kocher, B.; Stock, F.; Reifferscheid, G. Tyre and road wear particles (TRWP) - a review of generation, properties, emissions, human health risk, ecotoxicity, and fate in the environment. *Sci. Total. Environ.* **2020**, *733*, 137823. [DOI PubMed](#)
2. Zhang, Z. F.; Zhang, X.; Sverko, E.; et al. Determination of diphenylamine antioxidants in wastewater/biosolids and sediment. *Environ. Sci. Technol. Lett.* **2020**, *7*, 102-10. [DOI](#)

3. Tian, Z.; Zhao, H.; Peter, K. T.; et al. A ubiquitous tire rubber-derived chemical induces acute mortality in coho salmon. *Science* **2021**, *371*, 185-9. DOI PubMed
4. Wang, B.; Sun, W.; Ye, X.; Liu, Z.; Zhang, H. Occurrence, analytical methods, and ecotoxicological effects of 6PPD-Quinone in aquatic environments: a review. *TrAC. Trends. Anal. Chem.* **2025**, *193*, 118449. DOI
5. Zhang, Y.; Xu, C.; Zhang, W.; et al. *p*-Phenylenediamine antioxidants in PM_{2.5}: the underestimated urban air pollutants. *Environ. Sci. Technol.* **2021**, *56*, 6914-21. DOI PubMed
6. Li, Z.; Kannan, K. Occurrence of 1,3-diphenylguanidine, 1,3-di-*o*-tolylguanidine, and 1,2,3-triphenylguanidine in indoor dust from 11 countries: implications for human exposure. *Environ. Sci. Technol.* **2023**, *57*, 6129-38. DOI PubMed PMC
7. Rahman, M. M.; Shaikh, M. N. Synthesis and properties of cross-linkable waterborne polyurethane/HMMM-CNT nanocomposite. *Nano. Hybrids.* **2014**, *7*, 87-111. DOI
8. Sorce, F. S.; Shields, T.; Ngo, S.; Lowe, C.; Taylor, A. C. The effect of varying molecular weight on the performance of HMMM-crosslinked polyester coatings. *Prog. Org. Coat.* **2020**, *149*, 105920. DOI
9. Jin, R.; Li, B.; Wu, Y.; et al. Unpuzzling spatio-vertical and multi-media patterns of aniline accelerators/antioxidants in an urban estuary. *Water. Res.* **2024**, *266*, 122427. DOI PubMed
10. Zhang, H.; Huang, Z.; Liu, Y.; et al. Occurrence and risks of 23 tire additives and their transformation products in an urban water system. *Environ. Int.* **2023**, *171*, 107715. DOI PubMed
11. Wu, Y.; Venier, M.; Hites, R. A. Broad exposure of the North American environment to phenolic and amino antioxidants and to ultraviolet filters. *Environ. Sci. Technol.* **2020**, *54*, 9345-55. DOI PubMed
12. Cao, G.; Wang, W.; Zhang, J.; et al. New evidence of rubber-derived quinones in water, air, and soil. *Environ. Sci. Technol.* **2022**, *56*, 4142-50. DOI PubMed PMC
13. Zeng, L.; Li, Y.; Sun, Y.; Liu, L.; Shen, M.; Du, B. Widespread occurrence and transport of *p*-phenylenediamines and their quinones in sediments across urban rivers, estuaries, coasts, and deep-sea regions. *Environ. Sci. Technol.* **2023**, *57*, 2393-403. DOI PubMed
14. Wei, L. N.; Wu, N. N.; Xu, R.; et al. First evidence of the bioaccumulation and trophic transfer of tire additives and their transformation products in an Estuarine Food Web. *Environ. Sci. Technol.* **2024**, *58*, 6370-80. DOI PubMed
15. Zheng, G.; Boor, B. E.; Schreder, E.; Salamova, A. Indoor exposure to per- and polyfluoroalkyl substances (PFAS) in the childcare environment. *Environ. Pollut.* **2020**, *258*, 113714. DOI PubMed
16. Zheng, G.; Filippelli, G. M.; Salamova, A. Increased indoor exposure to commonly used disinfectants during the COVID-19 pandemic. *Environ. Sci. Technol. Lett.* **2020**, *7*, 760-5. DOI PubMed PMC
17. Singh, M. P.; Bhattacharyya, S.; Chinu, K.; Akter, R.; Marjo, C. E. Airborne soil and dust are potential sources of antimony to residents across Delhi: exposure likely to occur via dermal route. *Hyg. Environ. Health. Adv.* **2023**, *7*, 100075. DOI
18. Huang, W.; Shi, Y.; Huang, J.; et al. Occurrence of substituted *p*-phenylenediamine antioxidants in dusts. *Environ. Sci. Technol. Lett.* **2021**, *8*, 381-5. DOI
19. Zhu, J.; Guo, R.; Jiang, S.; Wu, P.; Jin, H. Occurrence of *p*-phenylenediamine antioxidants (PPDs) and PPDs-derived quinones in indoor dust. *Sci. Total. Environ.* **2024**, *912*, 169325. DOI PubMed
20. Tan, H.; Yang, L.; Huang, Y.; Tao, L.; Chen, D. "Novel" synthetic antioxidants in house dust from multiple locations in the Asia-Pacific region and the United States. *Environ. Sci. Technol.* **2021**, *55*, 8675-82. DOI PubMed
21. Ginsberg, G.; Toal, B.; Kurland, T. Benzothiazole toxicity assessment in support of synthetic turf field human health risk assessment. *J. Toxicol. Environ. Health. A.* **2011**, *74*, 1175-83. DOI PubMed
22. Liu, Z.; Feng, Y.; Sun, W.; et al. Environmental concentrations of 6PPD and 6PPD-quinone induce hepatic lipid metabolism disorders in male black-spotted frogs. *J. Hazard. Mater.* **2024**, *480*, 136400. DOI PubMed
23. Dejonckheere, G.; Herman, A.; Baeck, M. Allergic contact dermatitis caused by synthetic rubber gloves in healthcare workers: sensitization to 1,3-diphenylguanidine is common. *Contact. Dermatitis.* **2019**, *81*, 167-73. DOI PubMed
24. Dsikowitzky, L.; Schwarzbauer, J. Hexa(methoxymethyl)melamine: an emerging contaminant in German Rivers. *Water. Environ. Res.* **2015**, *87*, 461-9. DOI PubMed
25. Chang, J.; Zhang, L.; Zhao, J.; et al. 6PPD, not 6PPD-quinone, induced serious zebrafish eye damage by disrupting the thyroid signaling pathway. *Environ. Sci. Technol.* **2024**, *58*, 22076-88. DOI PubMed
26. Cheng, J.; Zhu, J.; Liu, Y.; Hua, J.; Li, S. Research progress on analytical methods for the determination of *p*-phenylenediamine-based rubber antioxidants and their quinone transformation products. *Chin. J. Chromatogr.* **2025**, *43*, 868-80. DOI
27. Banerjee, P.; Kemmler, E.; Dunkel, M.; Preissner, R. ProTox 3.0: a webserver for the prediction of toxicity of chemicals. *Nucleic. Acids. Res.* **2024**, *52*, W513-20. DOI PubMed PMC
28. Li, X.; Zhou, S.; Zhang, T.; et al. Occurrence and environmental fate/behaviors of tire wear particles and their human and ecological health: an emerging global issue. *Arch. Toxicol.* **2025**, *99*, 4353-66. DOI PubMed

29. USEPA. Exposure Factors Handbook (2011 Edition). <https://www.epa.gov/expobox/exposure-factors-handbook-2011-edition>. (accessed 2026-05-20).
30. USEPA. Update for Chapter 5 of the Exposure Factors Handbook: soil and dust ingestion. 2017. https://www.epa.gov/sites/default/files/2018-01/documents/efh-chapter05_2017.pdf. (accessed 2026-05-20).
31. Wang, Y. L.; Tsou, M. C. M.; Pan, K. H.; et al. Estimation of soil and dust ingestion rates from the stochastic human exposure and dose simulation soil and dust model for children in Taiwan. *Environ. Sci. Technol.* **2021**, *55*, 11805-13. DOI PubMed
32. Jin, R.; Wu, Y.; He, Q.; et al. Ubiquity of amino accelerators and antioxidants in road dust from multiple land types: targeted and nontargeted analysis. *Environ. Sci. Technol.* **2023**, *57*, 10361-72. DOI PubMed
33. Sartori, L.; Beaud, J.; Rime, C.; et al. Occurrence and toxicological risk characterization of 6-PPD, 6-PPDQ, and related rubber-associated chemicals in fruits and vegetables. *J. Hazard. Mater.* **2026**, *502*, 140988. DOI PubMed
34. Liu, C.; Wan, S.; Cheng, Y.; et al. Occurrence, sources, and human exposure assessment of amine-based rubber additives in dust from various micro-environments in South China. *Sci. Total. Environ.* **2024**, *955*, 177023. DOI PubMed
35. Breider, F.; Masset, T.; Prud'homme, K.; Brüscheweiler, B. J. Assessment of tire-derived additives and their metabolites into fruit, root and leafy vegetables and evaluation of dietary intake in Swiss adults. *J. Hazard. Mater.* **2025**, *494*, 138432. DOI PubMed
36. Mao, T.; Liu, W.; Deng, J.; et al. p-Phenylenediamines and p-phenylenediamine quinone derivatives in rubber consumer products and typical urban dust: sources, transformation profiles, and health risks. *Environ. Int.* **2024**, *192*, 109042. DOI PubMed
37. Xu, Q.; Li, G.; Fang, L.; et al. Enhanced formation of 6PPD-Q during the aging of wear particles in anaerobic flooded soils: the role of iron reduction and environmentally persistent free radicals. *Environ. Sci. Technol.* **2023**, *57*, 5978-87. DOI PubMed
38. Zhang, R.; Zhao, S.; Liu, X.; et al. Aquatic environmental fates and risks of benzotriazoles, benzothiazoles, and p-phenylenediamines in a catchment providing water to a megacity of China. *Environ. Res.* **2023**, *216*, 114721. DOI PubMed
39. USEPA. ChemView. <https://chemview.epa.gov/chemview/>. (accessed 2026-05-20).
40. ECHA. European Chemicals Agency. <https://echa.europa.eu/>. (accessed 2026-05-20).
41. Hiki, K.; Yamamoto, H. Concentration and leachability of N-(1,3-dimethylbutyl)-N'-phenyl-p-phenylenediamine (6PPD) and its quinone transformation product (6PPD-Q) in road dust collected in Tokyo, Japan. *Environ. Pollut.* **2022**, *302*, 119082. DOI PubMed
42. Tian, Z.; Gonzalez, M.; Rideout, C. A.; et al. 6PPD-quinone: revised toxicity assessment and quantification with a commercial standard. *Environ. Sci. Technol. Lett.* **2022**, *9*, 140-6. DOI
43. Zhao, H. N.; Hu, X.; Gonzalez, M.; et al. Screening p-phenylenediamine antioxidants, their transformation products, and industrial chemical additives in crumb rubber and elastomeric consumer products. *Environ. Sci. Technol.* **2023**, *57*, 2779-91. DOI PubMed
44. Avagyan, R.; Sadiqtis, I.; Bergvall, C.; Westerholm, R. Tire tread wear particles in ambient air - a previously unknown source of human exposure to the biocide 2-mercaptobenzothiazole. *Environ. Sci. Pollut. Int.* **2014**, *21*, 11580-6. DOI PubMed
45. Zhang, J.; Zhang, X.; Wu, L.; et al. Occurrence of benzothiazole and its derivatives in tire wear, road dust, and roadside soil. *Chemosphere* **2018**, *201*, 310-7. DOI PubMed
46. Xu, A.; Brillas, E.; Han, W.; Wang, L.; Sirés, I. On the positive effect of UVC light during the removal of benzothiazoles by photoelectro-Fenton with UVA light. *Appl. Catal. B. Environ.* **2019**, *259*, 118127. DOI
47. ECHA. 1,3-Diphenylguanidine (EC Number: 203-002-1, CAS Number: 102-06-7) REACH Dossier. European Chemicals Agency, 2020. <https://echa.europa.eu/documents/10162/4df27360-03aa-3c93-54f0-08f8366f42f3>. (accessed 2026-05-20).
48. Enroth, J.; Saarikoski, S.; Niemi, J.; et al. Chemical and physical characterization of traffic particles in four different highway environments in the Helsinki metropolitan area. *Atmos. Chem. Phys.* **2016**, *16*, 5497-512. DOI
49. Hiller, E.; Pilková, Z.; Filová, L.; Jurkovič, E.; Mihaljevič, M.; Lacina, P. Concentrations of selected trace elements in surface soils near crossroads in the city of Bratislava (the Slovak Republic). *Environ. Sci. Pollut. Res.* **2020**, *28*, 5455-71. DOI PubMed
50. Sieber, R.; Kaweckı, D.; Nowack, B. Dynamic probabilistic material flow analysis of rubber release from tires into the environment. *Environ. Pollut.* **2020**, *258*, 113573. DOI PubMed
51. Cao, G.; Wang, W.; Zhang, J.; et al. Occurrence and fate of substituted p-phenylenediamine-derived quinones in Hong Kong wastewater treatment plants. *Environ. Sci. Technol.* **2023**, *57*, 15635-43. DOI PubMed PMC
52. Rodovalho, E. D. C.; De Tomı, G. Reducing environmental impacts via improved tyre wear management. *J. Clean. Prod.* **2017**, *141*, 1419-27. DOI
53. Ricarte, M.; Prats, E.; Montemurro, N.; et al. Environmental concentrations of tire rubber-derived 6PPD-quinone alter CNS function in zebrafish larvae. *Sci. Total. Environ.* **2023**, *896*, 165240. DOI PubMed
54. Ding, Y.; Wang, W. Tissue-specific bioaccumulation and hepatotoxicity of 6PPD and 6PPD-Quinone in zebrafish. *Environ. Chem. Ecotoxicol.* **2026**, *8*, 307-18. DOI
55. Sherman, A.; Hämmerle, L. E.; Ben Mordechay, E.; Chefetz, B.; Hüffer, T.; Hofmann, T. Uptake of tire-derived compounds in leafy vegetables and implications for human dietary exposure. *Front. Environ. Sci.* **2024**, *12*, 1384506. DOI

-
56. Zhao, H. N.; Thomas, S. P.; Zylka, M. J.; Dorrestein, P. C.; Hu, W. Urine excretion, organ distribution, and placental transfer of 6PPD and 6PPD-quinone in mice and potential developmental toxicity through nuclear receptor pathways. *Environ. Sci. Technol.* **2023**, *57*, 13429-38. [DOI PubMed PMC](#)

Disclaimer/Publisher's Note: All statements, opinions, and data contained in this publication are solely those of the individual author(s) and contributor(s) and do not necessarily reflect those of OAE and/or the editor(s). OAE and/or the editor(s) disclaim any responsibility for harm to persons or property resulting from the use of any ideas, methods, instructions, or products mentioned in the content.



© The Author(s) 2026. Open Access This article is licensed under a Creative Commons Attribution 4.0 International License (<https://creativecommons.org/licenses/by/4.0/>), which permits unrestricted use, sharing, adaptation, distribution and reproduction in any medium or format, for any purpose, even commercially, as long as you give appropriate credit to the original author(s) and the source, provide a link to the Creative Commons license, and indicate if changes were made.